Hindawi
Advances in Civil Engineering
Volume 2020, Article ID 8870928, 9 pages
https://doi.org/10.1155/2020/8870928

Research Article

Stability Analysis of Surrounding Rock in Circular Tunnels Based on Critical Support Pressure

Hao Fan, Lianguo Wang, and Kai Wang

State Key Laboratory for Geomechanics and Deep Underground Engineering, China University of Mining and Technology, Xuzhou 221116, China

Correspondence should be addressed to Lianguo Wang; cumt_lgwang@163.com

Received 31 July 2020; Revised 9 September 2020; Accepted 24 September 2020; Published 16 October 2020

Academic Editor: Xun Xi

Accurate calculation for the critical support pressure of tunnels plays an important role in tunnel stability evaluation and support design. In this study, a mechanical model for circular tunnels is developed. Considering the intermediate principal stress and strain-softening characteristic of rock mass, the critical support pressure when the plastic zone and damage zone begin to occur is determined based on the unified strength criterion and strain-softening model. Through the example study, the critical support pressure under different intermediate principal stress coefficient is solved. Furthermore, the effect of initial field stress, softening coefficient, and maximum damage variable on the critical support pressure are also discussed. The results show that the critical support pressure and radii of plastic and damage zones all decrease with the increase of the intermediate principal stress coefficient. The larger the initial field stress, the larger the critical support pressure. The softening coefficient and maximum damage variable of rock mass has no influence on the critical support pressure when the plastic zone begins to form, but has a significant effect on the critical support pressure when the damage zone begins to form. As softening coefficient increases and maximum damage variable decreases, the critical support pressure when the damage zone which begins to form increases. Data presented in this contribution provide significant theoretical insights into evaluating tunnel stability and support system reliability.

1. Introduction

Tunnels are widely used in civil engineering, traffic engineering, and mining engineering [1, 2]. The excavation of the tunnels leads to the redistribution of the in situ stress. Once the redistributed stress is greater than the peak strength of the rock mass, the surrounding rock will be deformed and destroyed [3]. Generally, the surrounding rock around the tunnel suffers from the most severe damage, and this part is called the damage zone. The deep rock mass is still in an elastic state, which is called the elastic zone. And the transition from the failure zone to the elastic zone is called the plastic zone. Therefore, the range of the plastic zone and damage zone is very important to the design of the tunnel support system [4–6].

Strength criterion is the key to solving the radius of the plastic zone of the tunnel. In early work, linear Mohr–Coulomb strength criterion [7–10], nonlinear Hoek–Brown strength criterion [11–13], and generalized Hoek–Brown strength criterion [14–16] were used to analyzing the stresses distribution and deformations. However, the effect of intermediate principal stress on the surrounding rock was ignored by these criteria. A large number of test results show that the strength of rock mass is not only related to its own mechanical properties but also controlled by its stress state [17–22]. In practice, the underground rock mass is still in a triaxial stress state due to the existence of the supporting structure. Therefore, it is expected that the elastic-plastic analysis of tunnels should take the intermediate principal stress into consideration [23]. The unified strength criterion reasonably considers the influence of intermediate principal stress and is well suitable for many materials [24–27]. Thus, the unified strength criterion was chosen to analyze the tunnels in this study.

After the excavation of the tunnel, if enough support pressure can be applied to replace the excavated rock mass, the roadway will remain in a balanced state. However, if the support pressure is relatively small, the tunnel will suffer from different degrees of deformation [28]. Therefore, finding out the critical support pressure is of great significance for maintaining the stability of the tunnel surrounding rock. In the present study, a mechanical model of the circular tunnel was firstly established. Then, the critical support pressure when the plastic zone and damage zone begin to form is determined based on the strain-softening model and unified strength criterion. Finally, the sensitivity of the geomechanical parameters on the critical support pressure is discussed.

2. Problem Description

2.1. Mechanical Model of Circular Tunnels. An infinitely circular tunnel was excavated in uniform rock mass subjected to an initial field stress (p_0) at infinity boundary and a support pressure (p_i) at the tunnel surface (Figure 1). After excavation, there appeared the elastic zone, plastic zone, and damage zone around the tunnel. And the radii of the plastic and damage zones are denoted by R_p and R_d, respectively.

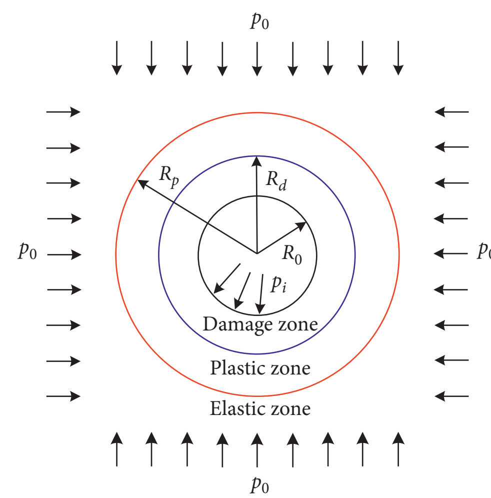

Figure 1: Mechanical model of the circular tunnel.

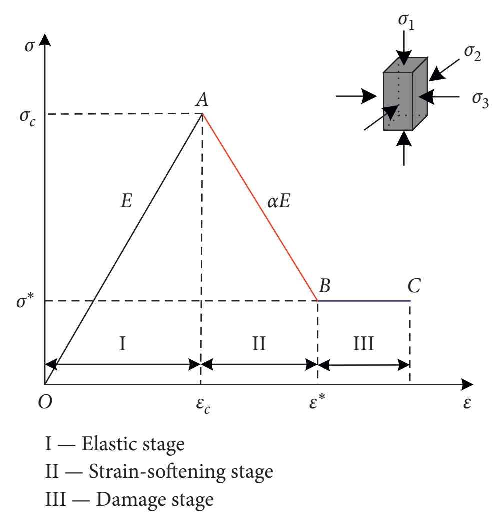

Figure 2: Simplified strain-softening model of the rock mass.

2.2. Strain-Softening Model of the Rock Mass. As shown in Figure 2, the rock mass has gone through an elastic stage (OA), a strain-softening stage (AB), and a residual strength stage (BC) during the whole failure process. The elastic modulus in the elastic stage and softening modulus in the strain-softening stage are denoted by E and αE, respectively, where α is the softening coefficient. The elastic stage, strain-softening stage, and residual strength stage of the full stress-strain curve correspond to the elastic zone, plastic zone, and damage zone of the surrounding rock in circular tunnels, respectively.

According to damage theory, the relationship between stress σ and strain ε of rock mass when considering damage can be written as

$$\sigma = (1 - D)E\varepsilon, \tag{1}$$

where D is the damage variable.

In one-dimensional case, the damage variable can be expressed as

$$\begin{cases} D = 0, & \varepsilon < \varepsilon_c, \\ D = \alpha\left(\dfrac{\varepsilon}{\varepsilon_c} - 1\right), & \varepsilon_c < \varepsilon \leq \varepsilon^*, \\ D = D_{\max}, & \varepsilon \geq \varepsilon, \end{cases} \tag{2}$$

where ε_c is the maximum elastic strain. ε^* is the strain when the rock mass enters the residual strength stage. $D_{\max}$ is the maximum damage variable.

In the three-dimensional case, the equivalent strain (ε_i) can be expressed as

$$\varepsilon_i = \frac{\sqrt{2}}{3}\sqrt{\left(\varepsilon_1 - \varepsilon_2\right)^2 + \left(\varepsilon_2 - \varepsilon_3\right)^2 + \left(\varepsilon_3 - \varepsilon_1\right)^2}. \tag{3}$$

By using the equivalent strain instead of uniaxial strain, the damage variable in the plastic zone can be obtained as

$$D = \frac{\lambda}{E}\left(\frac{\varepsilon_i}{\varepsilon_c} - 1\right). \tag{4}$$

2.3. Unified Strength Criterion. Assuming that the compressive stress is positive and the tensile stress is negative, the unified strength criterion can be expressed as

$$\begin{cases} \sigma_1 - \dfrac{(1+\sin\phi)(b\sigma_2+\sigma_3)}{(1+b)(1-\sin\phi)} = \dfrac{2c\cos\phi}{1-\sin\phi}, & \sigma_2 \le \dfrac{\sigma_1+\sigma_3}{2} - \dfrac{\sigma_1-\sigma_3}{2}\sin\phi, \\ \dfrac{\sigma_1+b\sigma_2}{1+b} - \dfrac{(1+\sin\phi)\sigma_3}{1-\sin\phi} = \dfrac{2c\cos\phi}{1-\sin\phi}, & \sigma_2 \ge \dfrac{\sigma_1+\sigma_3}{2} - \dfrac{\sigma_1-\sigma_3}{2}\sin\phi, \end{cases} \tag{5}$$

where c and φ are the cohesion and internal friction angle of the rock mass, respectively. σ_1, σ_2, and σ_3 are the maximum, intermediate, and minimum principal stresses, respectively. b is the intermediate principal stress coefficient. When $b = 0$, the unified strength criterion degenerates to the Mogi–Coulomb strength criterion; when $b = 1$, the unified strength criterion degenerates to the general twin shear strength criterion; when $0 < b < 1$, the unified strength criterion degenerates to a series of other new strength criteria.

Under plane strain conditions, the following can be easily obtained:

$$\sigma_z = \mu(\sigma_r + \sigma_\theta), \tag{6}$$

where μ is Poisson's ratio.

The radial stress (σ_r), axial stress (σ_z), and tangential stress (σ_θ) in the surrounding rock of a tunnel can be regarded as σ_1, σ_2, and σ_3, respectively. Therefore, the unified strength criterion can be rewritten as

$$\sigma_\theta - A\sigma_r - B = 0, \tag{7}$$

where

$$\begin{aligned} A &= \frac{1+b-b\mu+\sin\phi(-1b+b\mu)}{(1-\sin\phi)(b\mu+1)}, \\ B &= \frac{2c\cos\phi(1+b)}{(1-\sin\phi)(b\mu+1)}. \end{aligned} \tag{8}$$

3. Elastic-Plastic Analysis of the Surrounding Rock

The excavation of the tunnel results in the redistribution of the stresses in the surrounding rock mass. When the redistributed stress is less than the peak strength of the rock mass, the surrounding rock only undergoes elastic deformation. When the redistributed stress is greater than the peak strength of the rock mass, the surrounding rock undergoes plastic damage and the bearing capacity decrease. The damage degree of the rock mass increases with the increase of stress until it enters the residual strength stage. At this time, a damage zone appears around the surrounding rock.

3.1. Plastic Zone Begins to Form.

The equilibrium differential equation in the plastic zone can be written as

$$\frac{d\sigma_r}{dr} + \frac{\sigma_r - \sigma_\theta}{r} = 0. \tag{9}$$

The geometric equation can be expressed as

$$\begin{aligned} \varepsilon_r &= \frac{du}{dr}, \\ \varepsilon_\theta &= \frac{u}{r}. \end{aligned} \tag{10}$$

According to the effective stress theory [29], the effective stress in the plastic zone meets the unified strength criterion. Therefore, equation (7) can be rewritten as

$$\sigma'_\theta - A\sigma'_r - B = 0, \tag{11}$$

where σ'_θ and σ'_r are the effective radial stress and tangential stress, respectively.

Assuming that the damage of the surrounding rock is isotropic, the effective stresses can be expressed as

$$\begin{aligned} \sigma'_\theta &= \frac{\sigma_\theta}{1-D}, \\ \sigma'_r &= \frac{\sigma_r}{1-D}, \end{aligned} \tag{12}$$

Substituting (12) in (11), the following can be obtained:

$$\frac{\sigma_\theta}{1-D} - A\frac{\sigma_r}{1-D} - B = 0. \tag{13}$$

In the plane strain state, assuming that the volume of the rock mass in the plastic zone is constant, therefore, the relationship between the radial and tangential strains can be given as

$$\varepsilon_r + \varepsilon_\theta = 0. \tag{14}$$

Combined with the boundary condition on the interface between the elastic and plastic zones, the equivalent strain can be deduced by superimposing (10) and (14):

$$\varepsilon_i = \frac{R_p^2}{r^2}\varepsilon_c. \tag{15}$$

Substituting (15) into (8), the damage variable can be rewritten as

$$D = \alpha\left(\frac{R_p^2}{r^2} - 1\right). \tag{16}$$

Combined with the boundary condition of $\sigma_r = p_i$ at $r = R_0$, the radial and tangential stresses in the plastic zone can be derived by substituting (13) and (16) into (9):

$$\begin{cases} \sigma_r = B\left(\dfrac{p_i}{B} + \dfrac{1+\alpha}{A-1} - \dfrac{\alpha}{A+1}\dfrac{R_p^2}{R_0^2}\right)\left(\dfrac{r}{R_0}\right)^{A-1} - B\left(\dfrac{1+\alpha}{A-1} - \dfrac{\alpha}{A+1}\dfrac{R_p^2}{r^2}\right), \\ \sigma_\theta = A\sigma_r + B\left(1+\alpha-\alpha\dfrac{r_p^2}{r^2}\right). \end{cases} \tag{17}$$

According to the elasticity theory [30], an assumed stress function is given as

$$\Phi = M\ln r + Nr^2, \tag{18}$$

where M and N are the constants. The radial and tangential stresses are then given by

$$\begin{aligned} \sigma_r &= \frac{1}{r}\frac{d\Phi}{dr} = \frac{M}{r^2} + 2N, \\ \sigma_\theta &= \frac{d^2\Phi}{dr^2} = -\frac{M}{r^2} + 2N. \end{aligned} \tag{19}$$

Substituting the boundary conditions $\sigma_{re} = p_0$ at $r \longrightarrow \infty$ and $\sigma_{re} = \sigma_{\mathrm{rep}}$ at $r = R_p$ into (19), where σ_{rep} is the radial stress on the interface between the elastic and plastic zones, (19) can be rewritten as

$$\begin{aligned} \sigma_r &= \sigma_{\mathrm{rep}}\frac{R_p^2}{r^2} + p_0\left(1 - \frac{R_p^2}{r^2}\right), \\ \sigma_\theta &= -\sigma_{\mathrm{rep}}\frac{R_p^2}{r^2} + p_0\left(1 + \frac{R_p^2}{r^2}\right). \end{aligned} \tag{20}$$

Combining with (7) and (20), the radial stress on the interface between the elastic and plastic zones can be deduced as

$$\sigma_{\mathrm{rep}} = \frac{2p_0 - B}{A+1}. \tag{21}$$

Substituting (21) into (17), the following equation can be obtained:

$$\begin{aligned} \frac{2p_0 - B}{A+1} = {} & B\left(\frac{p_i}{B} + \frac{1+\alpha}{A-1} - \frac{\alpha}{A+1}\frac{R_p^2}{R_0^2}\right)\left(\frac{R_p}{R_0}\right)^{A-1} \\ & - B\left(\frac{1+\alpha}{A-1} - \frac{\alpha}{A+1}\right). \end{aligned} \tag{22}$$

The value of R_p can be derived by solving (22). Then, the stresses distribution in the elastic and plastic zones can be obtained by introducing the value of R_p into (17) and (20).

3.2. Damage Zone Begins to Form. In the damage zone, equation (7) can be rewritten as

$$\sigma_\theta = A\sigma_r + B\left(1 - D_{\max}\right). \tag{23}$$

Combined with the boundary condition of $\sigma_r = p_i$ at $r = R_0$, the radial and tangential stresses in the damage zone can be derived by substituting (23) into (9):

$$\begin{cases} \sigma_r = \dfrac{B\left(1-D_{\max}\right)}{1-A} + \left(p_i - \dfrac{B\left(1-D_{\max}\right)}{1-A}\right)\left(\dfrac{r}{R_0}\right)^{A-1}, \\ \sigma_\theta = \dfrac{B\left(1-D_{\max}\right)}{1-A} + A\left(p_i - \dfrac{B\left(1-D_{\max}\right)}{1-A}\right)\left(\dfrac{r}{R_0}\right)^{A-1}. \end{cases} \tag{24}$$

The radial stress on the interface between the plastic and damage zones σ_{rpd} can be derived by combining (23) and (24):

$$\sigma_{rpd} = \frac{B\left(1-D_{\max}\right)}{1-A} + \left(p_i - \frac{B\left(1-D_{\max}\right)}{1-A}\right)\left(\frac{R_d}{R_0}\right)^{A-1}. \tag{25}$$

According to (17), the stresses in the plastic zone can be obtained as

$$\begin{cases} \sigma_r = B\left(\dfrac{\sigma_{rpd}}{B} + \dfrac{1+\alpha}{A-1} - \dfrac{\alpha}{A+1}\dfrac{R_p^2}{R_d^2}\right)\left(\dfrac{r}{R_d}\right)^{A-1} - B\left(\dfrac{1+\alpha}{A-1} - \dfrac{\alpha}{A+1}\dfrac{R_p^2}{r^2}\right), \\ \sigma_\theta = A\sigma_r + B\left(1+\alpha-\alpha\dfrac{R_p^2}{r^2}\right). \end{cases} \tag{26}$$

Combined with (2), (16), and (23), the relationship between R_p and R_d can be derived as

$$R_p = R_d \sqrt{1 + \frac{D_{\max}}{\alpha}}. \tag{27}$$

Considering the continuity of radial stress in the elastic and plastic zones, the following equation can be obtained:

$$B\left(\frac{\sigma_{rpd}}{B} + \frac{1+\alpha}{A-1} - \frac{\alpha}{A+1}\frac{R_p^2}{R_d^2}\right)\left(\frac{R_p}{R_d}\right)^{A-1} - B\left(\frac{1+\alpha}{A-1} - \frac{\alpha}{A+1}\right) = \frac{2p_0 - B}{A+1}. \tag{28}$$

The value of R_p and R_d can be expressed by combining (25), (27), and (28):

$$R_d = R_0 \cdot \left(\frac{(((2p_0/B - 1 - \alpha)/A + 1) + ((1+\alpha)/(A-1)))(\alpha/(\alpha + D_{\max}))^{((A-1)/2)} + (((\alpha + D_{\max})/(A+1)) - ((\alpha + D_{\max})/(A-1)))}{(p_i/B) + ((1 - D_{\max})/(A-1))}\right)^{(1/(A-1))},$$

$$R_p = R_0 \cdot \left(\frac{(((2p_0/B - 1 - \alpha)/A + 1) + ((1+\alpha)/(A-1)))(\alpha/\alpha + D_{\max})^{((A-1)/2)} + (((\alpha + D_{\max})/(A+1)) - ((\alpha + D_{\max})/(A-1)))}{(p_i/B) + ((1 - D_{\max})/(A-1))}\right)^{(1/A-1)} \cdot \left(1 + \frac{D_{\max}}{\alpha}\right)^{(1/2)}. \tag{29}$$

The stresses distribution in the elastic, plastic, and damage zones can be obtained by introducing (29) into (24), (26), and (20).

3.3. Determination of the Critical Support Pressure. According to (29), when the support pressure reaches a certain value, the rock mass will be in the critical state.

When $p_i = p_{i1}$, the surrounding rock is in the critical state that the plastic zone begins to form. Then, the following equations can be obtained:

$$\begin{cases} \sigma_r = p_i \dfrac{R_0^2}{r^2} + p_0\left(1 - \dfrac{R_0^2}{r^2}\right), \\ \sigma_\theta = -p_i \dfrac{R_0^2}{r^2} + p_0\left(1 + \dfrac{R_0^2}{r^2}\right). \end{cases} \tag{30}$$

The critical support pressure (p_{i1}) can be derived by combining (7) and (30):

$$p_{i1} = \frac{2p_0 - B}{A+1}. \tag{31}$$

When $p_i = p_{i2}$, the surrounding rock is in the critical state that the damage zone begins to form. Combining the boundary condition of $\sigma_r = p_i$ at $r = R_0$ and (16), the relationship between R_p and R_0 can be written as

$$R_p = R_0 \sqrt{1 + \frac{D_{\max}}{\alpha}}. \tag{32}$$

The critical support pressure (p_{i2}) can be derived by substituting (32) into (22):

$$p_{i2} = \left(\frac{2p_0 - B(1+\alpha)}{A+1} + \frac{B(1+\alpha)}{A-1}\right) \cdot \left(\frac{\alpha}{\alpha + D_{\max}}\right)^{((A-1)/2)} + B\left(\frac{\alpha + D_{\max}}{A+1} - \frac{1+\alpha}{A-1}\right). \tag{33}$$

4. Example Study

4.1. Case I: Stress Distribution around the Tunnel. Taking a circular tunnel with the radius $R_0 = 2.5$ m as an example, the initial field stress is 15 MPa. The elastic modulus of the rock mass is 1350 MPa, softening coefficient is 2, cohesion is 2.5 MPa, internal friction angle is 30°, Poisson's ratio is 0.3, and maximum damage variable is 70%.

The critical support pressure under different intermediate principal stress coefficients is shown in Table 1. Take $b = 0.5$ as an example, the stress distribution under different support pressures is shown in Figure 3. It can be seen that when $p_i \geq 4.783$ MPa, the tunnel surrounding rock only consists of the elastic zone. When $2.632 \leq p_i < 4.783$ MPa, the plastic zone begins to form, and then, the tunnel surrounding rock is composed of the elastic and plastic zones. Once $p_i < 2.632$ MPa, the damage zone begins to develop and the tunnel surrounding rock finally displays three zones: elastic zone, plastic zone, and damage zone.

Figure 4 shows the stresses distribution under different intermediate principal stress coefficients when the support pressure is 1 MPa. It can be seen that as b increases, the whole radial stress, the tangential stress in the damage and plastic zones, and the peak tangential stress all show an increase, while the tangential stress in the elastic zone and the radii of the plastic and damage zones show a decrease. For example, as b transforms from 0 to 1, the peak tangential stress increases by 1 MPa, and the R_p and R_d values decrease by 0.639 m and 0.550 m, respectively. Therefore, the intermediate principal stress should be properly considered in engineering applications.

4.2. Case II: Effect of Parameters on the Critical Support Pressure

4.2.1. Effect of the Initial Field Stress. The influence of initial field stress on the critical support pressure under different intermediate principal stress coefficients is shown in Figure 5. It can be seen that the initial field stress has a significant influence on the critical support pressure. The p_{i1}

Table 1: Critical support pressure under different intermediate principal stress coefficients.

b	p_{i1}	p_{i2}
0	5.338	3.226
0.25	5.044	2.912
0.5	4.783	2.632
0.75	4.549	2.380
1	4.339	2.152

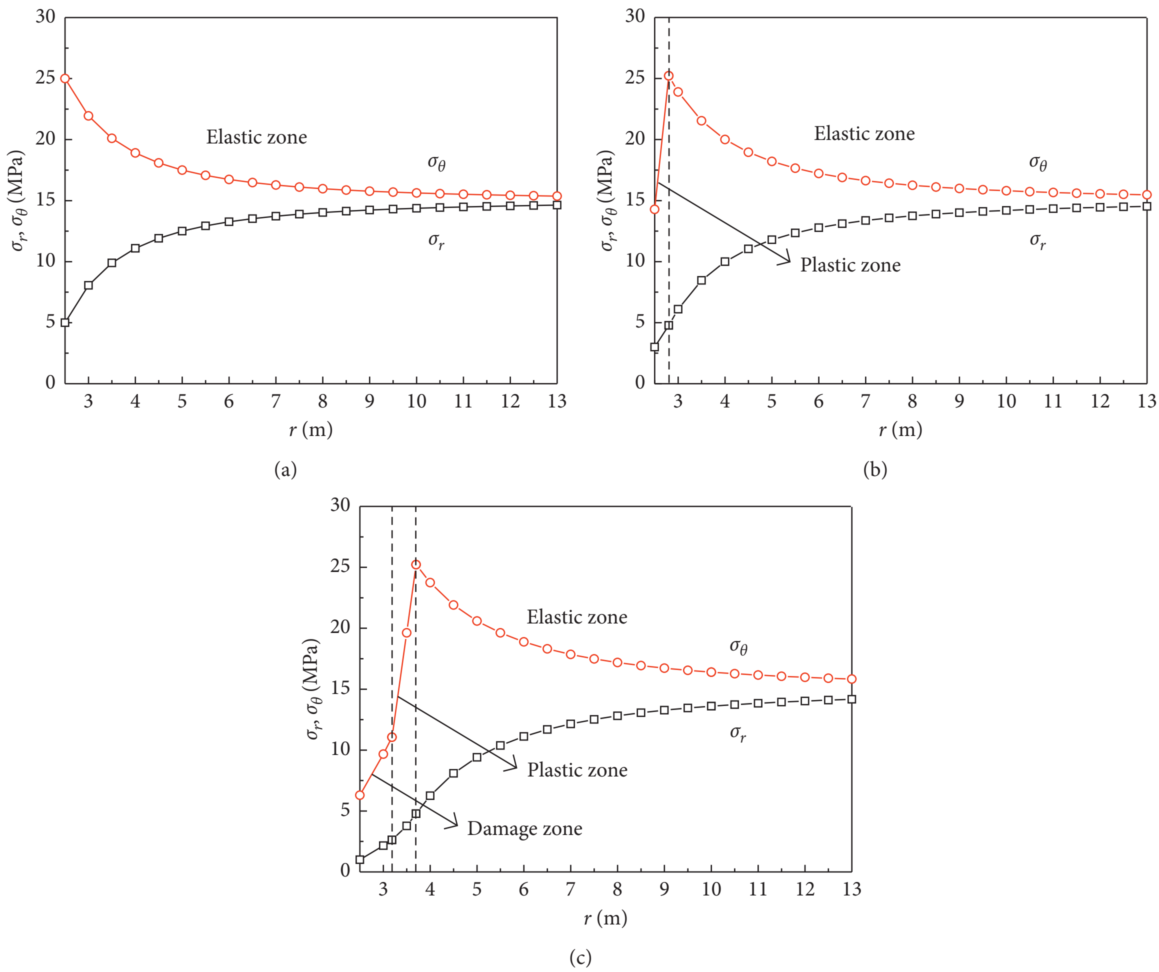

Figure 3: Stresses distribution under different support pressures. (a) $p_i = 5$ MPa, (b) $p_i = 3$ MPa, and (c) $p_i = 1$ MPa.

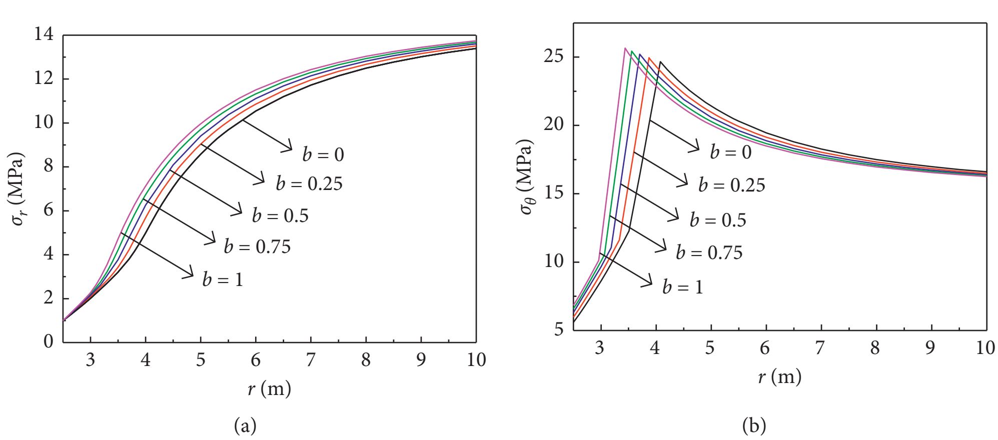

Figure 4: Stresses distribution under different intermediate principal stress coefficients. (a) σ_r and (b) σ_θ.

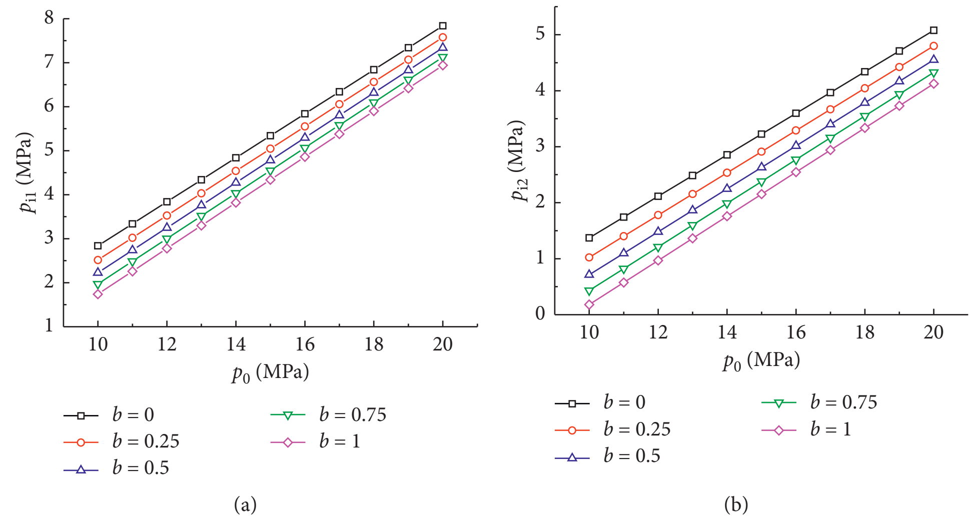

FIGURE 5: Influence of initial field stress on the critical support pressure under different intermediate principal stress coefficients. (a) p_{i1} and (b) p_{i2}.

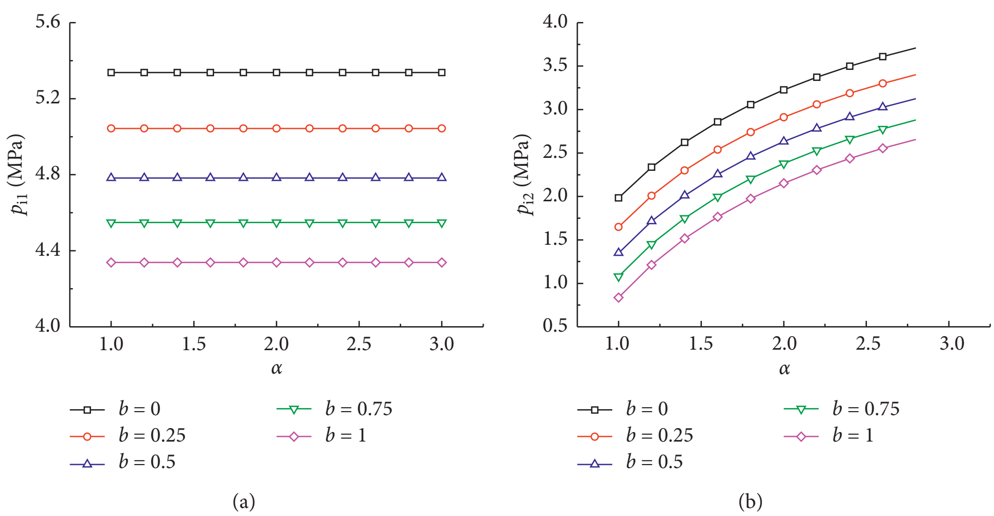

FIGURE 6: Influence of the softening coefficient on the critical support pressure under different intermediate principal stress coefficients. (a) p_{i1} and (b) p_{i2}.

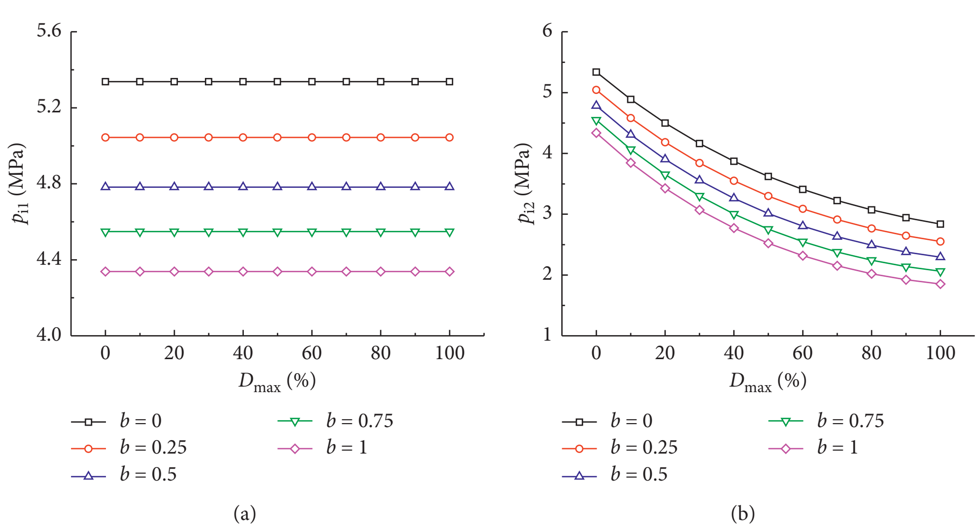

FIGURE 7: Influence of the maximum damage variable on the critical support pressure under different intermediate principal stress coefficients. (a) p_{i1} and (b) p_{i2}.

and p_{i2} values both increase with increasing p_0. Take $b = 0.5$ as an example, as p_0 increases from 10 MPa to 20 MPa, p_{i1} and p_{i2} values increase by 5.113 MPa and 3.839 MPa, with an increment of 229.69% and 539.19%, respectively. Therefore, as the depth of the tunnel increases, greater support force needs to be applied to maintain the stability of the tunnel surrounding rock.

4.2.2. Effect of the Softening Coefficient. The influence of the softening coefficient on the critical support pressure under different intermediate principal stress coefficients is shown in Figure 6. It can be seen that the softening coefficient has a significant effect on the critical support pressure (p_{i2}) when the damage zone begins to form. Take $b = 0.5$ as an example, as α increases from 1.0 to 3.0, the value of p_{i2} transforms from 1.349 MPa to 3.216 MPa, with an increment of 138.40%. However, but the softening coefficient has no effect on the critical support pressure (p_{i1}) when the plastic zone begins to form.

4.2.3. Effect of the Maximum Damage Variable. Figure 7 shows the sensitivity of the maximum damage variable to the critical support pressure under different intermediate principal stress coefficients. It can be seen that the maximum damage variable has no influence on the value of p_{i1}. However, the value of p_{i2} shows an increase with the continuous increase of the maximum damage variable. Take $b = 0.5$ as an example; as $D_{\max}$ increases from 0 to 100%, the value of p_{i2} decreases by 2.249 MPa, with a reduction of 55.52%. The results show that the lighter the damage degree of the rock mass, the more difficult it is for the tunnel surrounding rock to appear damage zone. Therefore, some measures, such as grouting, can be used to reduce the damage degree of the rock mass and ensure tunnel stability.

5. Conclusions

A mechanical model of the circular tunnel was firstly established. Considering the strain-softening characteristics of rock mass, the critical support pressure when the plastic zone and damage zone begin to form was deduced based on the unified strength criterion. The stress distribution under different support pressures and different intermediate principal stress coefficients were analyzed. The effects of initial field stress, softening coefficient, and maximum damage variable on the critical support pressure were discussed. The conclusions can be summarized as follows:

(1) The critical support pressure and radii of plastic and damage zones all decrease with the increase of critical support pressure and the stress coefficient. Therefore, the support design should take the intermediate principal stress into consideration.

(2) The critical support pressure increase with increasing initial field stress. Therefore, as the depth of the tunnel increases, greater support force needs to be applied to maintain the stability of the tunnel surrounding rock.

(3) The softening coefficient and maximum damage variable of rock mass has no influence on the critical support pressure when the plastic zone begins to form, but has a significant effect on the critical support pressure when the damage zone begins to form. With the softening coefficient increasing, the p_{i2} value increases. However, the p_{i2} value decreases as maximum damage variable increases. Therefore, tunnel stability can be effectively controlled by reducing the damage degree of the rock mass.

Data Availability

All data generated or analyzed during this study are included in this published article.

Conflicts of Interest

The authors declare that they have no conflicts of interest.

Acknowledgments

Financial support from the National Key Research and Development Program of China (no. 2017YFC0603004) and China Postdoctoral Science Foundation funded project (no. 2020M671649) are gratefully acknowledged.

References

[1] Q. Guo, J. Pan, X. Wu, X. Xi, and M. Cai, "A new unified solution for circular tunnels based on generalized SMP criterion considering the strain softening and dilatancy," *Advances in Civil Engineering*, vol. 2019, Article ID 1684707, 10 pages, 2019.

[2] H. Fan, L. Wang, and W. Liu, "An analytical solution for stresses and deformations of tunnels in a non-uniform stress field based on strain-softening model and Mogi-Coulomb criterion," *Latin American Journal of Solids and Structures*, vol. 17, no. 1, pp. 1–16, 2020.

[3] X. Xi, S. Yang, and C.-Q. Li, "A non-uniform corrosion model and meso-scale fracture modelling of concrete," *Cement and Concrete Research*, vol. 108, pp. 87–102, 2018.

[4] J. Pan, Q. Guo, F. Ren, and M. Cai, "Comparative analysis of different strength criteria for deep-buried rock roadway under seepage," *Journal of China Coal Society*, vol. 44, no. 11, pp. 3369–3378, 2019, in Chinese.

[5] A. Lv, H. Masoumi, S. D. C. Walsh, and H. Roshan, "Elastic-softening-plasticity around a borehole: an analytical and experimental study," *Rock Mechanics and Rock Engineering*, vol. 52, no. 4, pp. 1149–1164, 2019.

[6] A. Ghorbani and H. Hasanzadehshooiili, "A comprehensive solution for the calculation of ground reaction curve in the crown and sidewalls of circular tunnels in the elastic-plastic-EDZ rock mass considering strain softening," *Tunnelling and Underground Space Technology*, vol. 84, pp. 413–431, 2019.

[7] K.-H. Park and Y.-J. Kim, "Analytical solution for a circular opening in an elastic-brittle-plastic rock," *International Journal of Rock Mechanics and Mining Sciences*, vol. 43, no. 4, pp. 616–622, 2006.

[8] Y.-K. Lee and S. Pietruszczak, "A new numerical procedure for elasto-plastic analysis of a circular opening excavated in a

strain-softening rock mass," *Tunnelling and Underground Space Technology*, vol. 23, no. 5, pp. 588–599, 2008.

[9] S. Wang, X. Yin, H. Tang, and X. Ge, "A new approach for analyzing circular tunnel in strain-softening rock masses," *International Journal of Rock Mechanics and Mining Sciences*, vol. 47, no. 1, pp. 170–178, 2010.

[10] A. Singh, K. S. Rao, and R. Ayothiraman, "Effect of intermediate principal stress on cylindrical tunnel in an elasto-plastic rock mass," *Procedia Engineering*, vol. 173, pp. 1056–1063, 2017.

[11] Q. Zhang, B. Jiang, and H. Lv, "Analytical solution for a circular opening in a rock mass obeying a three-stage stress-strain curve," *International Journal of Rock Mechanics and Mining Sciences*, vol. 86, pp. 16–22, 2016.

[12] M. Fraldi and F. Guarracino, "Limit analysis of collapse mechanisms in cavities and tunnels according to the Hoek-Brown failure criterion," *International Journal of Rock Mechanics and Mining Sciences*, vol. 46, no. 4, pp. 665–673, 2009.

[13] S. K. Sharan, "Exact and approximate solutions for displacements around circular openings in elastic-brittle-plastic Hoek-Brown rock," *International Journal of Rock Mechanics and Mining Sciences*, vol. 42, no. 4, pp. 542–549, 2005.

[14] C. Carranza-Torres, "Elasto-plastic solution of tunnel problems using the generalized form of the Hoek-Brown failure criterion," *International Journal of Rock Mechanics and Mining Sciences*, vol. 41, no. S1, pp. 629–639, 2004.

[15] S. K. Sharan, "Analytical solutions for stresses and displacements around a circular opening in a generalized Hoek-Brown rock," *International Journal of Rock Mechanics and Mining Sciences*, vol. 45, no. 1, pp. 78–85, 2008.

[16] R. Chen and F. Tonon, "Closed-form solutions for a circular tunnel in elastic-brittle-plastic ground with the original and generalized hoek-Brown failure criteria," *Rock Mechanics and Rock Engineering*, vol. 44, no. 2, pp. 169–178, 2011.

[17] W. Liu, J. Liu, and C. Zhu, "Multi-scale effect of acoustic emission characteristics of 3D rock damage," *Arabian Journal of Geosciences*, vol. 12, no. 22, pp. 1–12, 2019.

[18] X. Xi, S. Yang, C.-Q. Li, M. Cai, X. Hu, and Z. K. Shipton, "Meso-scale mixed-mode fracture modelling of reinforced concrete structures subjected to non-uniform corrosion," *Engineering Fracture Mechanics*, vol. 199, pp. 114–130, 2018.

[19] Z. Li, L. Wang, Y. Lu, W. Li, and K. Wang, "Experimental investigation on the deformation, strength, and acoustic emission characteristics of sandstone under true triaxial compression," *Advances in Materials Science and Engineering*, vol. 2018, Article ID 5241386, 16 pages, 2018.

[20] X.-T. Feng, R. Kong, X. Zhang, and C. Yang, "Experimental study of failure differences in hard rock under true triaxial compression," *Rock Mechanics and Rock Engineering*, vol. 52, no. 7, pp. 2109–2122, 2019.

[21] H. Zhang, D. Elsworth, and Z. Wan, "Failure response of composite rock-coal samples," *Geomechanics and Geophysics for Geo-Energy and Geo-Resources*, vol. 4, no. 2, pp. 175–192, 2018.

[22] X. Xi, X. Wu, Q. Guo, and M. Cai, "Experimental investigation and numerical simulation on the crack initiation and propagation of rock with pre-existing cracks," *IEEE Access*, vol. 8, pp. 129636–129644, 2020.

[23] M. Zhu, Y. Yang, F. Gao, and J. Liu, "Analytical solution of tunnel surrounding rock for stress and displacement based on Lade–Duncan criterion," *Advances in Civil Engineering*, vol. 2018, no. 7, Article ID 5363658, 2018.

[24] L. Chen, X. Mao, Y. Chen, M. Li, Y. Hao, and D. Liu, "A new unified solution for circular tunnel based on a four-stage constitutive model considering the intermediate principal stress," *Advances in Civil Engineering*, vol. 2018, Article ID 7912062, 14 pages, 2018.

[25] J. Li, G. Ma, and M. Yu, "Penetration analysis for geo-material based on unified strength criterion," *International Journal of Impact Engineering*, vol. 35, no. 10, pp. 1154–1163, 2008.

[26] M. Yu, "The Effect of the Intermediate Principal stress on the ground response of circular openings in rock mass," *Rock Mechanics and Rock Engineering*, vol. 39, no. 2, pp. 169–181, 2006.

[27] C. Zhang, J. Zhao, Q. Zhang, and X. Hu, "A new closed-form solution for circular openings modeled by the Unified Strength Theory and radius-dependent Young's modulus," *Computers and Geotechnics*, vol. 42, pp. 118–128, 2012.

[28] B. Jiang, L. Wang, Y. Lu, S. Gu, and X. Sun, "Failure mechanism analysis and support design for deep composite soft rock roadway: a case study of the Yangcheng coal mine in China," *Shock and Vibration*, vol. 2015, Article ID 452479, 14 pages, 2015.

[29] M. C. He, H. H. Jing, and X. M. Sun, *Soft Rock Engineering Mechanics*, Science Press, Beijing, China, 2002.

[30] J. Pan, Z. Gao, and F. Ren, "Effect of strength criteria on surrounding rock of circular roadway considering strain softening and dilatancy," *Journal of China Coal Society*, vol. 43, no. 12, pp. 3293–3301, 2018, in Chinese.